

Spontaneous rectification and absolute negative mobility of inertial Brownian particles induced by gaussian potentials in steady laminar flows

Jian-Chun Wu¹ and Meng An²

¹*School of Physics and Electronic Information,
Shangrao Normal University, Shangrao 334001, China*

²*College of Mechanical and Electrical Engineering,
Shaanxi University of Science and Technology, Xi'an 710021, China*

(Dated: June 14, 2022)

Abstract

We study the transport of inertial Brownian particles in steady laminar flows in the presence of two-dimensional Gaussian potentials. Through extensive numerical simulations, it is found that the transport is sensitively dependent on the external constant force and the position of the Gaussian potential. Under specific parameter conditions, the system exhibits some interesting transport phenomena. In the absence of any external driving forces, the spontaneous rectification of the particles can be controlled by changing the position of the Gaussian potential. When the potential is at the center of the cellular flow, the particles move in a direction opposite to the constant force, i.e., exhibiting absolute negative mobility. Absolute negative mobility can be enhanced obviously by varying the system parameters. More importantly, we can observe the phenomenon of ANM in a wider range of the system parameters, which may pave the way to the implementation of related experiments.

PACS numbers: 05.60.-k, 05.45.-a

Keywords: Brownian particles, spontaneous rectification, absolute negative mobility

I. INTRODUCTION

Over the past several decades, the transport of Brownian particles in random environment has played a central role in statistical physics, aiming at obtaining energy from random fluctuations. Usually, Brownian particles diffusion freely or move in the direction of external force in free space. However, the transport may show counter-intuitive behavior in some nonequilibrium systems[1, 2]. In ratchet systems, the directed motion of Brownian particles can occur in the absence of external biases. These ratchet systems require some fundamental conditions[3]: nonlinearity, spatial or temporal asymmetry, and a zero-mean nonequilibrium driving. In order to study the related transport phenomena, researchers proposed some typical ratchet models corresponding to the type of nonequilibrium driving, they are rocking ratchets[4, 5], flashing ratchets[6–8], coupled ratchets [9, 10], entropic ratchets[11, 12], and so on.

When the system is perturbed by an static force, the transport may exhibit complicated behavior depending on the surrounding environments. Due to the interaction between Brownian particles and complex environments, the system may show a phenomenon of negative differential mobility (NDM)[13–20], i.e., the velocity-force relation showing a nonmonotonic behavior. More surprisingly, under specific conditions, the particles move in the direction opposite to the direction of the static force. This phenomenon in nonequilibrium systems is called absolute negative mobility (ANM). There are some earlier studies for realizing ANM in a variety of setups, such as semiconductor superlattices[21], coupled Brownian motors[22, 23], and well-designed geometric channels[24–26]. Shortly afterwards, ANM in some specific structures was also observed by choosing proper driving and coupling ways[27–29]. By embedding the spatial asymmetry into the particle shape, Hänggi and co-workers[30, 31] found that a classical ANM for elongated particles can be realized in two-dimensional separate channels. Machura and co-workers[32] studied the motion of inertial Brownian particles in one-dimensionl symmetric periodic potentials, and found that the phenomenon of ANM can be induced by thermal equilibrium fluctuations under the influence of both a time periodic and a constant, biasing driving force. Based on this work, there are a large number of extended studies for ANM under different conditions[33–41].

Recently, the phenomenon of ANM has been observed in steady laminar flows[42–45]. Sarracino and co-workers[42] studied the mobility of an inertial tracer in a two-dimensional

incompressible laminar flow and observed the phenomena of negative differential mobility and absolute negative mobility, where the velocity field played the key role in these non-linear behavior. By applying a one-dimensional periodic potential, Ai and co-workers[45] found that absolute negative mobility can be drastically enhanced by choosing appropriate phase and height of the potential. In this paper, we study the transport of inertial Brownian particles in steady laminar flows in the presence of Gaussian Potentials. Different from the previous studies[42–45], the present system can exhibit the phenomena of spontaneous rectification and absolute negative mobility, simultaneously. In the absence of any external forces, the Gaussian potential produces the asymmetry of the system and induces the directed transport of Brownian particles. When the potential is at the center of the cellular flow, absolute negative mobility can be dramatically enhanced in a wider range of the system parameters.

II. MODEL AND METHODS

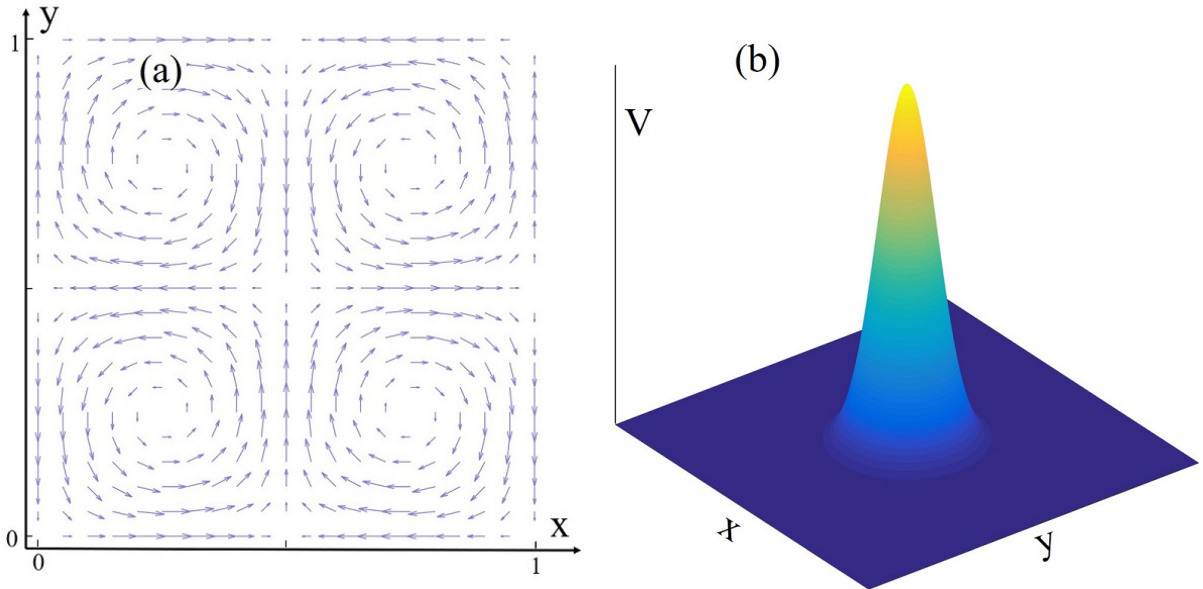


FIG. 1: Schematic of a divergenceless cellular flow and a Gaussian potential in a two-dimensional period. (a) The divergenceless cellular flow (U_x, U_y) is given by the stream-function $\varphi(x, y)$ in Eq.(5). (b) The Gaussian potential is described by Eq.(6).

We consider a two-dimensional system of size $L \times L$ with periodic boundary conditions,

see Fig. 1(a). In the system, an inertial particle with spatial coordinates (x, y) and velocities (v_x, v_y) moves in a divergenceless cellular flow (U_x, U_y) . The dynamics of the particle can be described by the following equations[42–45],

$$\frac{dx}{dt} = v_x, \quad (1)$$

$$\frac{dy}{dt} = v_y, \quad (2)$$

$$\frac{dv_x}{dt} = -\frac{1}{\tau}(v_x - U_x) + \frac{1}{m}(f + F_x) + \sqrt{2D}\xi_x, \quad (3)$$

$$\frac{dv_y}{dt} = -\frac{1}{\tau}(v_y - U_y) + \frac{1}{m}F_y + \sqrt{2D}\xi_y. \quad (4)$$

Here τ is the Stokes time, D denotes the diffusion coefficient. ξ_x and ξ_y model white Gaussian noises with zero mean and obey $\langle \xi_i(t)\xi_j(t') \rangle = \delta_{ij}\delta(t - t')$ for $i, j = x, y$. m is the mass of the inertial particle, and is set to 1 throughout the work. The divergenceless cellular flow $(U_x, U_y) = (\partial\varphi/\partial y, -\partial\varphi/\partial x)$ [46] and the stream-function $\varphi(x, y)$ has the form,

$$\varphi(x, y) = LU_0/(2\pi)\sin(2\pi x/L)\sin(2\pi y/L). \quad (5)$$

In this paper, the particle is subjected to the force field consists of two parts, a external constant force f along the x direction, and the substrate forces F_x and F_y from the Gaussian potentials,

$$V(x, y) = Ae^{-\varepsilon^2[(x-\Delta x)^2+(y-\Delta y)^2]}, \quad (6)$$

where A and ε control the strength and size of the potential, respectively. The region influenced by the potential decreases with the increaseing of ε . Δx and Δy are the spatial coordinates of the potential in a two-dimensional period, see Fig. 1(b).

In the following, we introduce the characteristic length L and time L/U_0 by setting $L = 1$ and $U_0 = 1$, respectively. For simplicity, we only investigate the transport of Brownian particles for the case of $\Delta y = 0.5$. In numerical simulations, we integrate Eqs. (1-4) by using the second-order stochastic Runge-Kutta algorithm with the time step and the total

integration time being 10^{-4} and 10^4 , respectively. Thus, the average velocity of particles along the x direction can be calculated as

$$\langle v_x \rangle = \lim_{t \rightarrow \infty} \frac{\langle x(t) - x(0) \rangle}{t}, \quad (7)$$

where $\langle \dots \rangle$ denotes the average over trajectories of the particle with random initial conditions and noise realizations.

III. RESULTS AND DISCUSSION

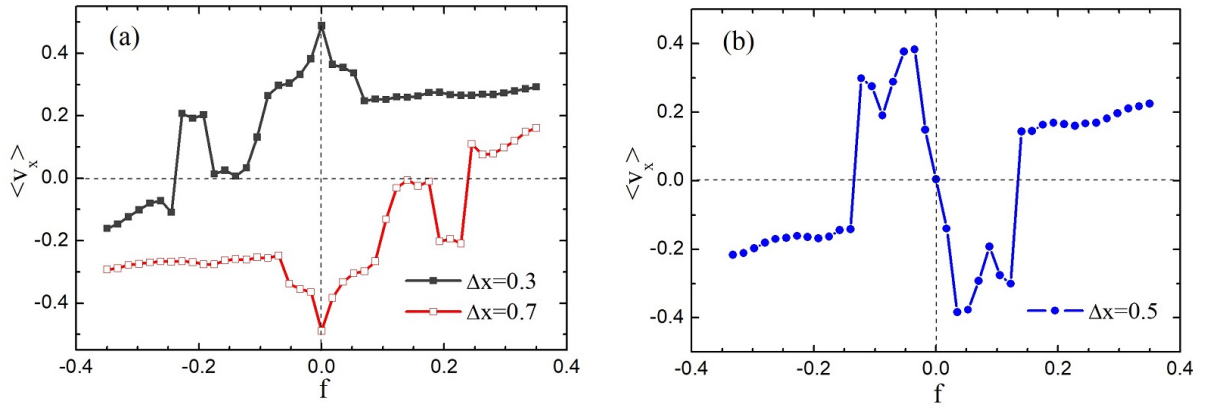


FIG. 2: Average velocity $\langle v_x \rangle$ as a function of the constant force f for different values of Δx . The parameters are chosen as $\varepsilon = 10.0$, $A = 1.0$, $D = 10^{-5}$ and $\tau = 1.0$.

In this section, we mainly explore how the spatial position of Gaussian potential affects the transport of inertial Brownian particles. We first plot the velocity-force curves for different values of Δx in Fig. 2. When the spatial position of the Gaussian potential is asymmetric in the cellular flow, e.g., $\Delta x = 0.3$, the transport exhibits a complex behavior due to the presence of the Gaussian potential and may reverse its direction by varying the constant force. When $\Delta x = 0.7$, the transport shows a completely opposite result compared to the case of $\Delta x = 0.3$, see Fig. 2(a). In the absence of any external force ($f = 0$), an interesting phenomenon of spontaneous rectification appears due to the presence of the system asymmetry induced by the Gaussian potential. However, when the Gaussian potential is at the center of the cellular flow ($\Delta x = 0.5$), the system exhibits the anomalous phenomenon of ANM, see Fig. 2(b). More remarkably, ANM can be dramatically enhanced

compared to the Refs.[42, 43, 45], and the range of f for the appearance of ANM is increased by a factor of 3 compared to the Ref.[45].

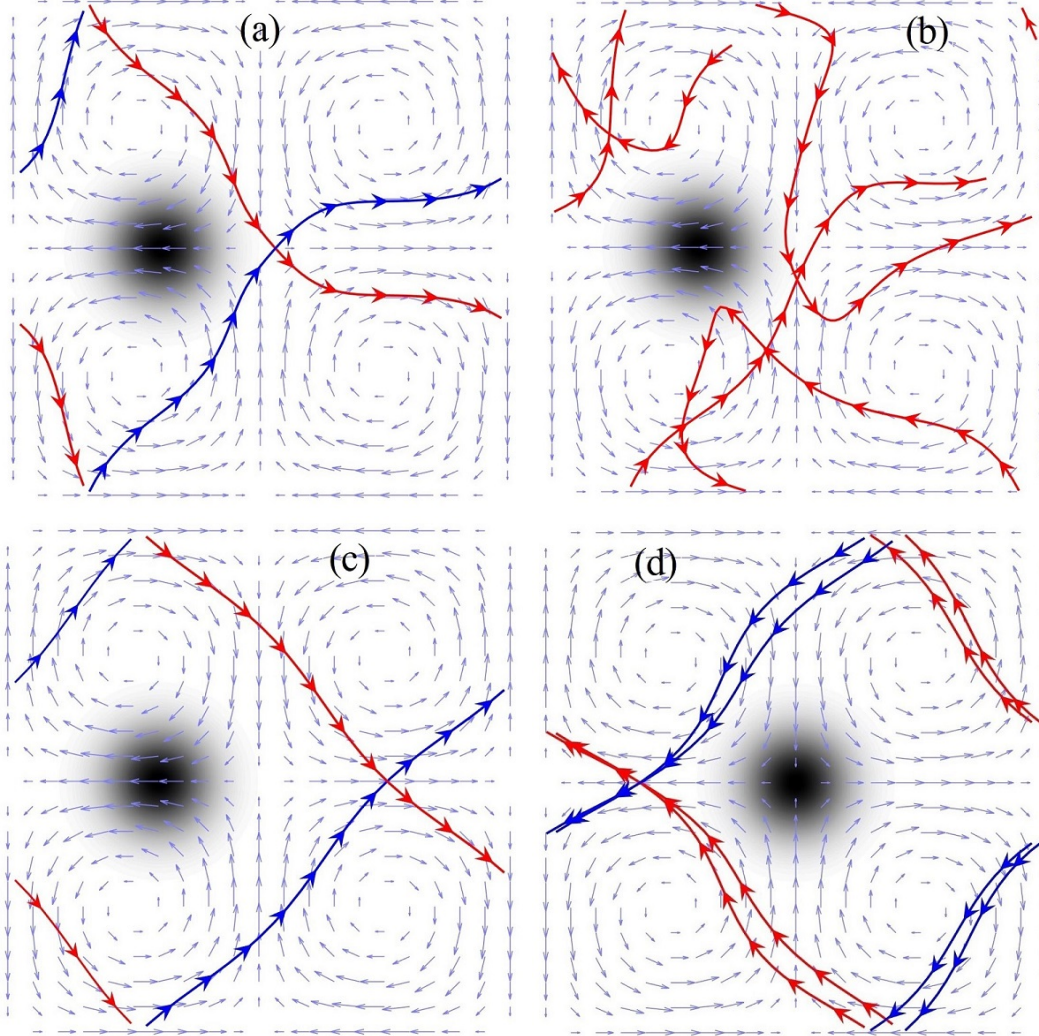


FIG. 3: Sample trajectories of a Brownian particle for different cases. (a) $f = -0.2$ and $\Delta x = 0.3$, (b) $f = -0.14$ and $\Delta x = 0.3$, (c) $f = 0.0$ and $\Delta x = 0.3$, and (d) $f = 0.05$ and $\Delta x = 0.5$. The other parameters are same as that in Fig. 2.

In order to understand the details of the transport, we plot the trajectories of inertial Brownian particles to explain the transport behavior shown in Fig. 2. From Fig. 3, there exist some preferential channels[42], and the particles may move along these paths depending on the potential position. We first analyse the case of $\Delta x = 0.3$ in Figs. 3(a-c). When $f = -0.2$, the Gaussian potential obstruct the movement of the particles in the $-x$ direction, meanwhile the divergenceless cellular flow guides the particles to move along the

two preferential channels shown in Fig. 3(a), thus the average velocity is positive. When $f = -0.14$, the particles frequently collide with the potential [see Fig. 3(b)], there are no preferential channels, thus the average velocity tends to zero. When $f = 0.0$, the Gaussian potential produces the asymmetry of the system, and provides two preferential channels shown in Fig. 3(c) for Brownian particles. Obviously, the trajectories in Fig. 3(c) is more directed compared to that in Fig. 3(a), and the average velocity approaches 0.5 [see Fig. 2(a)]. For the case of $\Delta x = 0.5$, the system asymmetry is completely determined by the constant force f . When $f = 0.05$, there exist two preferential channels shown in Fig. 3(d) in the movement process, thus the system exhibits the phenomenon of ANM.

The above results show apparent advantages over other papers[42, 43, 45]. Therefore, we should give more details about large enhancement. In the following, two specific cases will be discussed in detail: spontaneous rectification at $f = 0.0$ and absolute negative mobility at $\Delta x = 0.5$.

A. Spontaneous rectification

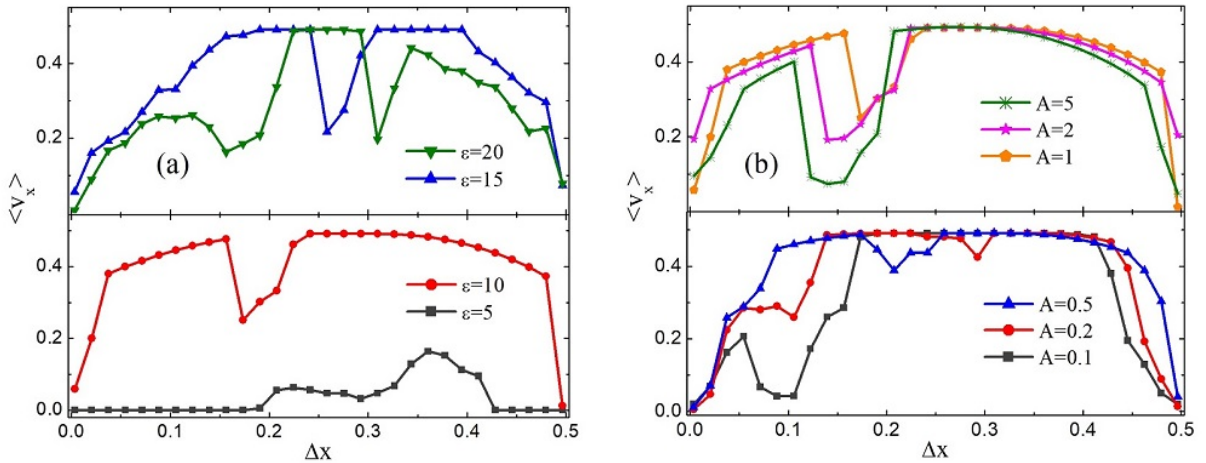


FIG. 4: (a) Average velocity $\langle v_x \rangle$ as a function of the position Δx for different values of ε at $A = 1.0$. (b) Average velocity $\langle v_x \rangle$ as a function of the position Δx for different values of A at $\varepsilon = 10.0$. The other parameters are chosen as $f = 0.0$, $D = 10^{-5}$ and $\tau = 1.0$.

Figure 4(a) shows the average velocity $\langle v_x \rangle$ as a function of the position Δx for different values of ε . When ε is very small, the Gaussian potential will overlap obviously with the

adjacent potentials, thus the particles may be trapped by these potentials. In the case of $\varepsilon = 5.0$, the region influenced by the potential is relatively large and the influence of the cellular flow on the rectification becomes weak, thus the average velocity $\langle v_x \rangle$ is small. With the increasing of ε , the region influenced by the potential decreases. When ε is very large, the effects of the potential can be neglected [not shown here]. In the case of $\varepsilon = 20.0$, the rectification effect on average is weak compared to the cases of $\varepsilon = 10.0$ and $\varepsilon = 15.0$, and the range of Δx for obtaining optimal $\langle v_x \rangle$ becomes small.

Figure 4(b) shows the average velocity $\langle v_x \rangle$ as a function of the position Δx for different values of A . It is found that the strength of the Gaussian potential mainly influences the rectification effects at some particular positions. When A is small, e.g., $A = 0.1$, the Gaussian potential have a significant effect on the rectification in the region of $0.15 < \Delta x < 0.45$. When A is large enough, e.g., $A > 1.0$, the region influenced by the potential increases slightly with the increasing of A , which may weaken the rectification effect.

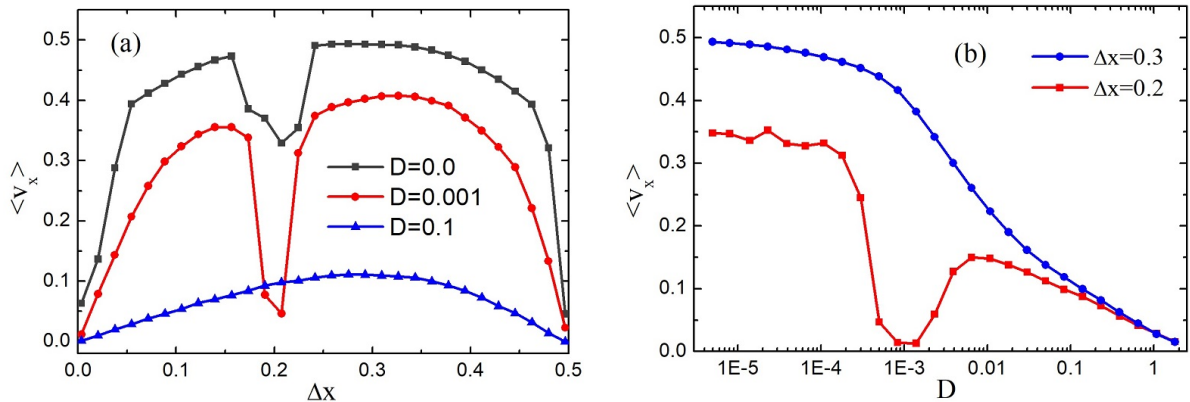


FIG. 5: (a) Average velocity $\langle v_x \rangle$ as a function of the position Δx for different values of D . (b) Average velocity $\langle v_x \rangle$ as a function of the diffusion coefficient D for different values of Δx . The parameters are chosen as $f = 0.0$, $\varepsilon = 10.0$, $A = 1.0$ and $\tau = 1.0$.

The average velocity $\langle v_x \rangle$ as a function of the position Δx is shown in Fig. 5(a) for different values of D . When $D = 0$, the system is deterministic, the average velocity $\langle v_x \rangle$ shows a nonmonotonic behavior with the increase of Δx . With the increasing of the diffusion coefficient D , the average velocity $\langle v_x \rangle$ decreases monotonically, see the case of $\Delta x = 0.3$ in Fig. 5(b). When D is large enough, e.g., $D = 0.1$, the average velocity $\langle v_x \rangle$ exhibits a nonmonotonic behavior with a bell shaped, there exists an optimized value of Δx at

which the average velocity takes its maximal value [see Fig. 5(a)]. However, for the case of $\Delta x = 0.2$ in Fig. 5(b), the average velocity $\langle v_x \rangle$ decreases first, then increases, and finally decreases to zero at very large D . Therefore, the environment noise may be benefit to the particle rectification under some specific conditions.

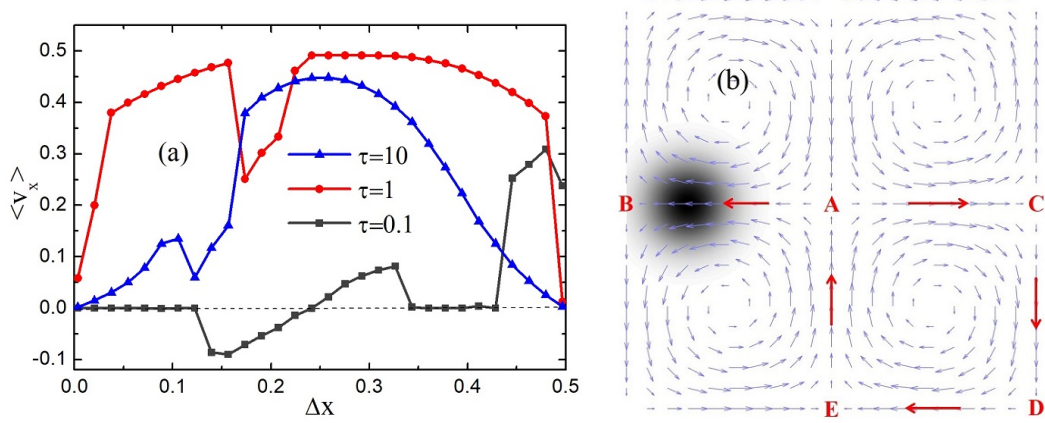


FIG. 6: (a) Average velocity $\langle v_x \rangle$ as a function of the position Δx for different values of τ . (b) Diagrammatic sketch illustrating the rectification of Brownian particles at $\tau = 0.1$ and $\Delta x = 0.15$, the red arrows indicate the possible direction of the particle movement. The parameters are chosen as $f = 0.0$, $\varepsilon = 10.0$, $A = 1.0$ and $D = 10^{-5}$.

Figure 6 shows the average velocity $\langle v_x \rangle$ as a function of the position Δx for different values of τ . It is found that the transport is sensitively dependent to the Stokes time. When the Stokes time is very small, e.g., $\tau = 0.1$, the cellular flow induces the particles to move along the velocity field and dominates the transport. Here, we mainly explain the transport in the case of $\Delta x = 0.15$. In Fig. 6(b), we plot the diagrammatic sketch at $\tau = 0.1$ and $\Delta x = 0.15$. We assume the point A is the initial position of the particle. Under the action of the cellular flow, the particles may move along the paths of $A \rightarrow B$ and $A \rightarrow C$. However, the particles can't move from the point C to the point B in adjacent cell due to the double obstructions from the cellular flow and Gaussian Potential. Then the particles may perform the movement along the path of $A \rightarrow C \rightarrow D \rightarrow E \rightarrow A$. Thus the average velocity $\langle v_x \rangle$ is negative. When the Stokes time is very large, e.g., $\tau = 10.0$, the effects of the cellular flow becomes weak and the average velocity on average decreases correspondingly compared to the case of $\tau = 1.0$.

B. Absolute negative mobility

In order to illustrate the effects of the Gaussian Potentials on the appearance of ANM, we plot the velocity-force curves and some contour plots of the average velocity versus the system parameters.

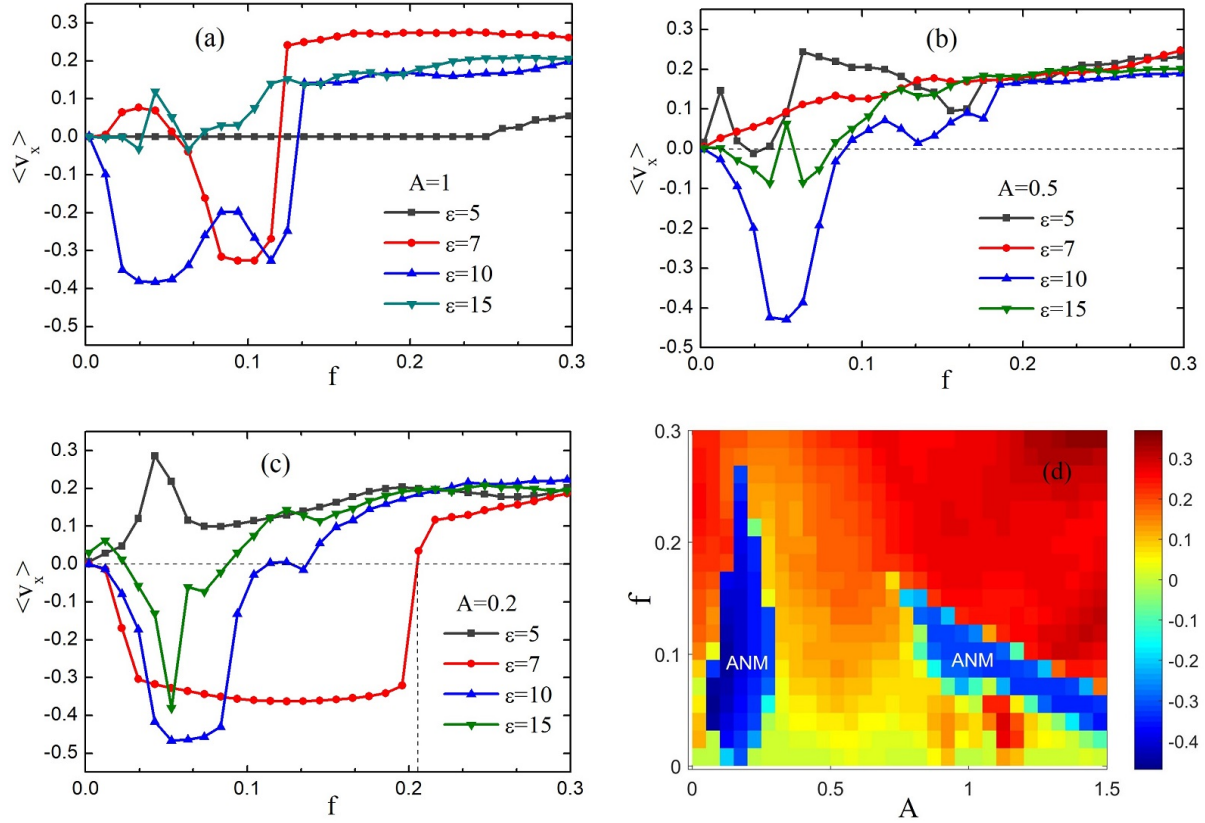


FIG. 7: Average velocity $\langle v_x \rangle$ as a function of the constant force f for different values of ε at (a) $A = 1.0$, (b) $A = 0.5$ and (c) $A = 0.2$. (d) Contour plots of the average velocity $\langle v_x \rangle$ versus A and f at $A = 0.2$ and $\varepsilon = 7.0$. The other parameters are chosen as $D = 10^{-5}$ and $\tau = 1.0$.

Figure 7(a) shows the average velocity $\langle v_x \rangle$ versus the constant force f for different values of ε at $A = 1.0$. It is found that the velocity-force relation is very complex. When ε is small, e.g., $\varepsilon = 5.0$, the particles may be trapped by the potentials in the divergenceless cellular flow for small constant force f . By increasing ε , one can observe the phenomenon of ANM in a certain range of f , see the cases of $\varepsilon = 7$ and $\varepsilon = 10$. When ε is large, e.g., $\varepsilon = 15.0$, the effect of the potential becomes weak, thus the ranges of f for observing ANM become small. Through numerical simulation, we find that the decreasing of A is beneficial to the

appearance of ANM under appropriate conditions. For the case of $A = 0.2$, see Fig. 7(c), the amplitude of ANM is greatly improved when $\varepsilon = 10.0$. And the range of f for observing ANM is further increased compared to that in Fig. 2(b).

In order to investigate the dependence of $\langle v_x \rangle$ on A and f in detail, we plot the contour plots $\langle v_x \rangle$ versus the strength of the potential A and the constant force f at $\varepsilon = 7.0$ in Fig. 7(d). There exist two regions for appearance of ANM. One can observe a more obvious phenomenon of ANM in the range of $0.05 < A < 0.3$ compared to the case of $A > 0.75$. In the following investigations, we will choose the parameters $0.05 < A < 0.3$ and $\varepsilon = 7.0$.

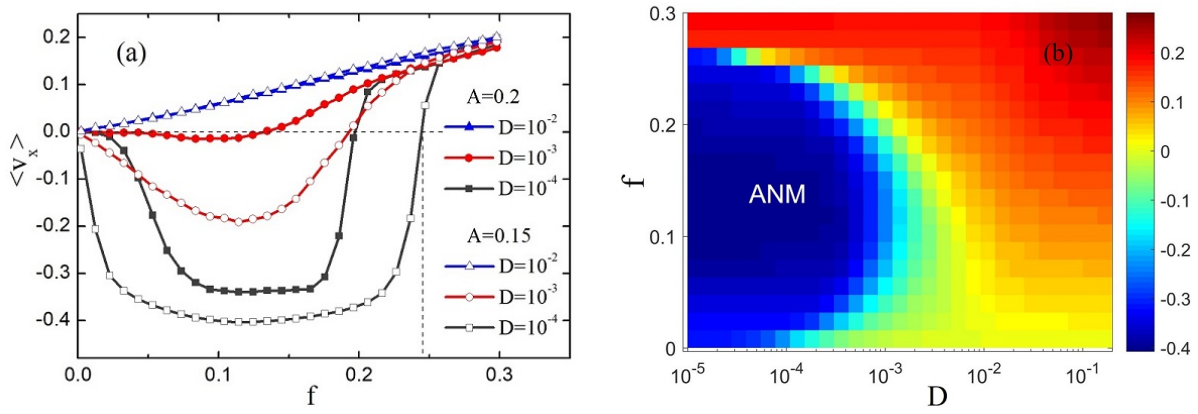


FIG. 8: (a) Average velocity $\langle v_x \rangle$ as a function of the constant force f for different values of (A, D) . (b) Contour plots of the average velocity $\langle v_x \rangle$ versus D and f at $A = 0.15$. The other parameters are chosen as $\varepsilon = 7.0$ and $\tau = 1.0$.

The random fluctuations may play an key role for the appearance of ANM[32], while suppress this phenomenon in steady laminar flows[42–45]. The dependence of $\langle v_x \rangle$ on the constant force f for different D is presented in Fig. 8(a). When the diffusion coefficient is large, e.g., $D = 0.01$, the average velocity $\langle v_x \rangle$ increases monotonically with the constant force f . When the diffusion coefficient is small enough, e.g., $D = 10^{-4}$ and 10^{-3} , a phenomenon of ANM can be observed. By contrast, a very obvious phenomenon of ANM can be observed by choosing $A = 0.15$. To show the dependence of $\langle v_x \rangle$ on D and f in more detail, we plot the contour plots $\langle v_x \rangle$ versus D and f at $A = 0.15$ in Fig. 8(b). It is found that ANM can occur in the case of $D < 0.004$ and the range of f for obtaining ANM increases with the decreasing of D . These results indicate that the random fluctuations may reduce

the nonequilibrium nature of the velocity field and a very obvious phenomenon of ANM appears in the absence of thermal equilibrium fluctuations [not shown here].

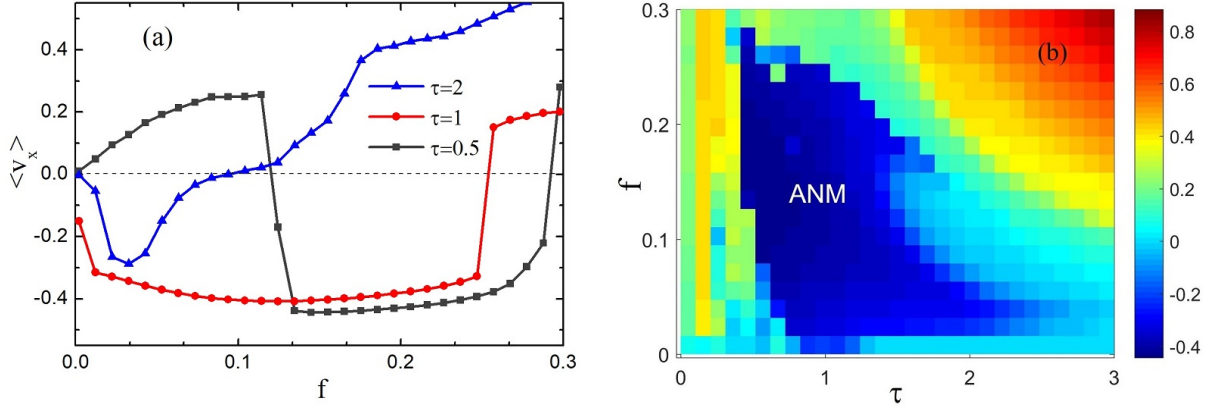


FIG. 9: (a) Average velocity $\langle v_x \rangle$ as a function of the constant force f for different values of τ . (b) Contour plots of the average velocity $\langle v_x \rangle$ versus τ and f . The other parameters are chosen as $A = 0.15$, $\varepsilon = 7.0$ and $D = 10^{-5}$.

In Fig. 9(a), we investigate the average velocity $\langle v_x \rangle$ versus the constant force f for different values of τ . It is found that a proper value of τ can promote the appearance of ANM, see the case of $\tau = 1.0$. Moreover, the range of f for the appearance of ANM is increased by a factor of 5 compared to the Ref.[45]. However, when the Stokes time is small or large, the range of f for ANM are both small, see the cases of $\tau = 0.5$ and $\tau = 2.0$. A detailed contour plots $\langle v_x \rangle$ versus τ and f are plotted in Fig. 9(b). It is found that ANM may occur in a range of $0.4 < \tau < 3.0$. When the Stokes time increases from 1.0 to 3.0, the range of f for ANM decreases.

IV. CONCLUDING REMARKS

In conclusion, we numerically investigated the transport of inertial Brownian particles induced by Gaussian potentials in steady laminar flows. We found that the transport is sensitively dependent on the external constant force for different positions of Gaussian potential. In the absence of any external driving forces, the Gaussian potential produces the asymmetry of the system and induce the spontaneous rectification of particles. The simulation results show that the rectification can be strongly enhanced by applying a proper

Gaussian potential and the average velocity can approach 0.5. Generally speaking, the average velocity decreases monotonically with the increasing of the diffusion coefficient, while exhibits a nonmonotonic behavior at particular position (e.g., $\Delta x = 0.2$). When the Stokes time is small ($\tau = 0.1$), the transport may reverse its direction under the combined action of the Gaussian Potential and the cellular flow. In addition, we also studied the velocity-force relation when the potential is at the center of the cellular flow. Under particular parameter conditions, the system exhibits the phenomenon of ANM. By adjusting the strength of the potential ($0.05 < A < 0.3$ and $A > 0.75$), absolute negative mobility occurs and the range of f for ANM is very large, e.g., $f < 0.2$ at $A = 0.2$ and $\varepsilon = 7.0$. When $A = 0.15$ and $\varepsilon = 7.0$, the effect of ANM can be further improved and the ranges of the parameters for the appearance of ANM are both very large, see Figs. 8(b) and 9(b).

This work was supported in part by the National Natural Science Foundation of China (Grant No. 11747109), the Natural Science Foundation of Jiangxi Province (Grant No. 20181BAB211011), the Science Foundation of Jiangxi Provincial Department of Education (Grant No. Gjj161057).

-
- [1] P. Hänggi and F. Marchesoni, Rev. Mod. Phys. 81, 387 (2009).
 - [2] P. Reimann, Phys. Rep. 361, 57 (2002).
 - [3] S. Denisov, P. Hänggi, and J. L. Mateos, Am. J. Phys. 77, 602 (2009).
 - [4] M. O. Magnasco, Phys. Rev. Lett. 71, 1477 (1993).
 - [5] R. Bartussek, P. Hänggi, J.G. Kissner, Europhys. Lett. 28, 459 (1994).
 - [6] R. D. Astumian and M. Bier, Phys. Rev. Lett. 72, 1766 (1994).
 - [7] M. Borromeo and F. Marchesoni, Phys. Lett. A 249, 199 (1998).
 - [8] J. D. Bao, Y. Z. Zhuo, Phys. Lett. A 239, 228 (1998).
 - [9] Z. Zheng, G. Hu, and B. Hu, Phys. Rev. Lett. 86, 2273 (2001).
 - [10] C. C. de Souza Silva, J. Van de Vondel, M. Morelle, and V. V. Moshchalkov, Nature (London) 440, 651 (2006).
 - [11] D. Reguera, G. Schmid, P. S. Burada, J. M. Rubi, P. Reimann, and P. Hänggi, Phys. Rev. Lett. 96, 130603 (2006).
 - [12] B. Q. Ai and J. C. Wu, J. Chem. Phys. 139, 034114 (2013).

- [13] R. L. Jack, D. Kelsey, J. P. Garrahan, and D. Chandler, *Phys. Rev. E* 78, 011506 (2008).
- [14] S. Leitmann and T. Franosch, *Phys. Rev. Lett.* 111, 190603 (2013).
- [15] U. Basu and C. Maes, *J. Phys. A* 47, 255003 (2014).
- [16] O. Bénichou, P. Illien, G. Oshanin, A. Sarracino, and R. Voituriez, *Phys. Rev. Lett.* 113, 268002 (2014).
- [17] O. Bénichou, P. Illien, G. Oshanin, A. Sarracino, and R. Voituriez, *Phys. Rev. E* 93, 032128 (2016).
- [18] M. Baiesi, A. L. Stella, and C. Vanderzande, *Phys. Rev. E* 92, 042121 (2015).
- [19] J. Cividini, D. Mukamel, and H. A. Posch, *J. Phys. A: Math. Theor.* 51, 085001 (2018).
- [20] A. K. Chatterjee, U. Basu, and P. K. Mohanty, *Phys. Rev. E* 97, 052137 (2018).
- [21] B. J. Keay, S. Zeuner, S. J. Allen, K. D. Maranowski, A. C. Gossard, U. Bhattacharya, and M. J. W. Rodwell, *Phys. Rev. Lett.* 75, 4102 (1995).
- [22] P. Reimann, R. Kawai, C. Van den Broeck, and P. Hänggi, *Europhys. Lett.* 45, 545 (1999).
- [23] B. Cleuren and C. Van den Broeck, *EPL* 54, 1 (2001).
- [24] R. Eichhorn, P. Reimann, and P. Hänggi, *Phys. Rev. Lett.* 88, 190601 (2002).
- [25] R. Eichhorn, P. Reimann, and P. Hänggi, *Phys. Rev. E* 66, 066132 (2002).
- [26] B. Cleuren and C. Van den Broeck, *Phys. Rev. E* 67, 055101(R) (2003).
- [27] R. Eichhorn, J. Regtmeier, D. Anselmetti, and R. Peter, *Soft Matter* 6, 1858 (2010).
- [28] D. Speer, R. Eichhorn, and P. Reimann, *Phys. Rev. Lett.* 102, 124101 (2009).
- [29] D. Speer, R. Eichhorn, M. Evstigneev, and P. Reimann, *Phys. Rev. E* 85, 061132 (2012).
- [30] P. Hänggi, F. Marchesoni, S. Savelev, and G. Schmid, *Phys. Rev. E* 82, 041121 (2010).
- [31] P. K. Ghosh, P. Hänggi, F. Marchesoni, and F. Nori, *Phys. Rev. E* 89, 062115 (2014).
- [32] L. Machura, M. Kostur, P. Talkner, J. Luczka, and P. Hänggi, *Phys. Rev. Lett.* 98, 040601 (2007).
- [33] J. Nagel, D. Speer, T. Gaber, A. Sterck, R. Eichhorn, P. Reimann, K. Ilin, M. Siegel, D. Koelle, and R. Kleiner, *Phys. Rev. Lett.* 100, 217001 (2008).
- [34] D. Hennig, *Phys. Rev. E* 79, 041114 (2009).
- [35] M. Kostur, J. Luczka, and P. Hänggi, *Phys. Rev. E* 80, 051121 (2009).
- [36] L. Du and D. Mei, *Phys. Rev. E* 85, 011148 (2012).
- [37] C. Mulhern, *Phys. Rev. E* 88, 022906 (2013).
- [38] J. Spiechowicz, P. Hänggi, and J. Luczka, *Phys. Rev. E* 90, 032104 (2014).

- [39] P. Magaretti, I. Pagonabarraga, and J. M. Rubi, *Phys. Rev. Lett.* 113, 128301 (2014).
- [40] B. Dandogbessi and A. Kenfack, *Phys. Rev. E* 92, 062903 (2015).
- [41] R. Chen, W. Pan, J. Zhang, and L. Nie, *Chaos* 26, 093113 (2016).
- [42] A. Sarracino, F. Cecconi, A. Puglisi, and A. Vulpiani, *Phys. Rev. Lett.* 117, 174501 (2016).
- [43] F. Cecconi, A. Puglisi, A. Sarracino, and A. Vulpiani, *Eur. Phys. J. E* 40, 81 (2017).
- [44] F. Cecconi, A. Puglisi, and A. Sarracino, *J. Phys.: Condens. Matter* 30, 264002 (2018).
- [45] B. Q. Ai, W. J. Zhu, Y. F. He, and W. R. Zhong, *J. Chem. Phys.* 149, 164903 (2018).
- [46] P. Tabeling, *Phys. Rep.* 362, 1 (2002).